

Imaging the Effects of Castration on Bone Turnover and Hormone-Independent Prostate Cancer Colonization of Bone

N.A. Cross,^{1*} A. Fowles,² K. Reeves,² N. Jokonya,² K. Linton,² I. Holen,²
F.C. Hamdy,² and C.L. Eaton²

¹Biomedical Research Centre, Sheffield Hallam University, Sheffield, UK

²Section of Urology, University of Sheffield Medical School, Sheffield, UK

INTRODUCTION. Tumor populations may selectively colonize bone that is being actively remodeled. In prostate cancer patients, androgen deprivation directly inhibits tumor growth initially, whilst induced bone loss may facilitate tumor colonization of bone by androgen-insensitive cells. We have tested this hypothesis using a xenograft model of early growth of prostate cancer in bone.

METHODS. PC3 cells transfected with Green fluorescent protein (GFP) were injected into castrated and non-castrated athymic mice via intratibial and intracardiac routes. In vivo tumor growth was monitored daily and animals sacrificed 6–9 days following initial GFP-based detection of tumors. Tumor bearing and contra-lateral non-tumor bearing tibias were analyzed extensively by micro-CT and histology/immunohistochemistry for the presence of tumor cells and the effects of tumor and/or castration on bone cells and bone structure evaluated.

RESULTS. GFP-positive tumors in bone were visible from 12 days post-injection following intratibial injection, allowing tumors <1 mm diameter to be monitored in live animals. Castration did not affect tumor frequency, tumor volume, or time to initial appearance of tumors injected via intratibial or intracardiac routes. Castration decreased trabecular bone volume in all mice. Significant tumor-induced suppression of numbers of osteoblasts, coupled with increased numbers of activated osteoclasts, was evident in both intact animals and castrated animals.

CONCLUSIONS. In vivo GFP imaging allows the detection of early tumor growth at intrasosseous sites. Castration induces bone loss, but PC3-GFP cells are also capable of inducing bone remodeling in intact animals at early time points, independently of pre-existing castration-induced alterations to bone. *Prostate* 68: 1707–1714, 2008. © 2008 Wiley-Liss, Inc.

KEY WORDS: androgens; osteolytic; osteoblast; osteoclast

INTRODUCTION

The development of skeletal metastases is a frequent occurrence in patients with advanced prostate cancer, a phenomenon that has a serious impact on morbidity and prognosis. Surveys [1,2] of the frequency and distribution of secondary disease in prostate cancer patients have shown that bone is the most common single site of metastasis as well as the overall most frequently colonized site. Since it is clear that prostate cancer cells gain access to the general circulation at an early stage [3], bone would seem to represent a preferred site of attachment survival and growth of disseminated prostate cancer cells. Studies of tumor

types that colonize the skeleton have suggested that tumor cells target areas of active bone turnover. This is evidenced by the observation that initial tumor growth

Abbreviations: GFP, green fluorescent protein; TRAP, tartrate resistant acid phosphatase.

Grant sponsor: MRC (PROMPT); Grant sponsor: European Union FP6 Award (PRIMA); Grant sponsor: Yorkshire Cancer Research.

*Correspondence to: Dr. N.A. Cross, Biomedical Research Centre, Sheffield Hallam University, Howard Street, Sheffield S1 1WB, UK.
E-mail: n.a.cross@shef.ac.uk

Received 20 December 2007; Accepted 8 July 2008

DOI 10.1002/pros.20833

Published online 25 August 2008 in Wiley InterScience
(www.interscience.wiley.com).

favors growth plates of long bones and the axial skeleton in general where bone turnover is more active. Other studies have shown experimentally, using in vivo models of prostate cancer growth in bone, that stimulation of bone turnover by agents such as parathyroid hormone (PTH) can enhance tumor colonization of bone [4]. Conversely, agents such as bisphosphonates that suppress bone turnover have been shown to inhibit tumor take rates in animals treated with these agents in conjunction with PTH [4]. In prostate cancer, castration, either surgical or pharmacological, is the major form of treatment for patients with locally advanced and/or metastatic disease. This approach suppresses the growth of hormone sensitive prostate cancer cells and in patients with skeletal metastases, alleviates symptoms in around 70% of patients. However, castration induced disease remission is inevitably followed by relapse and the development of androgen insensitive metastases. These can be at the original metastatic sites or at new foci. At this stage the disease is incurable and progressive. While there are undoubted benefits derived from castration in initially suppressing the growth of tumor cells themselves, the known effects of androgen ablation in increasing bone turnover could render the skeleton more receptive to colonization by tumor cells and even enhance their growth and survival in this environment. This would be particularly relevant to populations of these cells that were completely insensitive to androgens.

Studies of the processes involved in metastasis of prostate cancer cells to bone have been hampered by the limited availability of suitable in vivo models. Recent studies have used bioluminescence and fluorescence imaging of tumor cells in live animals to assess tumor burden, and the effects of therapeutic interventions on tumor growth in bone [5–7]. For the present study we have established our own in vivo model of prostate tumor cell growth in bone that stably expresses green fluorescent protein (GFP). We have shown that this model can be used to image the early events that occur during tumor colonization of bone, and tumors can be detected using GFP-imaging at much earlier stages of growth than described previously. We have used this model to test the hypothesis that castration of animals prior to tumor implantation enhances bone turnover in favor of bone loss, and increases tumor growth and the frequency of tumor colonization in bone.

MATERIALS AND METHODS

Cell Lines and Cultures

The human metastatic, androgen independent cell line PC3 was obtained from ATCC. Cells were cultured

in DMEM medium containing Glutamax (Invitrogen, Paisley, UK) supplemented with 10% Fetal calf serum (Invitrogen) and routinely grown in 5% CO₂ at 37°C. Cells were stably transfected with the pMaxGFP vector (Amaxa, Cologne, Germany) using an Amaxa transfection system. Colonies of GFP-positive PC3 cells were selected using 0.5 mg/ml Geneticin (Invitrogen). Cells used for this study were isolated from a single clone of GFP-positive cells. All cultures, including those isolated from experimental xenografts were confirmed negative of mycoplasma spp. infection using EZ-PCR mycoplasma system (Geneflow, Staffordshire, UK).

In Vivo Procedures

PC3-GFP cells were harvested when 80% confluent and detached using trypsin/EDTA. All procedures were performed on male MF1 athymic mice (aged 6–8 weeks) (Harlan laboratories, Bicester, UK). For subcutaneous injections, mice were injected with 1×10^6 cells in a volume of 100 μ l into the left flank. For intracardiac injections, mice were anaesthetized with Isoflurane and 1×10^5 cells injected directly into the left ventricle. Intratibial injections were performed using a modification of the method of Corey [8]. During surgery, mice were anaesthetized using 1–2% Isoflurane. An incision was made in front of the right tibia and two holes drilled into the bone marrow cavity using a 27-gauge needle. The bone marrow cavity was then flushed with sterile saline prior to injection of 10 μ l of culture medium containing 1.5×10^5 PC3-GFP cells. Finally, holes in the bone were filled with bone wax. Prior to closure, the area was washed with sterile water to lyse any tumor cells that spilled out of the holes in the bone, thus reducing the incidence of sub-cutaneous contamination and extraosseous tumor growth. In separate experiments, further groups of 12 animals were divided into two groups of 6 and one group surgically castrated 2 weeks prior to implantation of both groups with PC3-GFP cells via intracardiac or intratibial implantation.

In Vivo Monitoring of Tumor Growth

Mice were monitored daily by whole body fluorescence imaging using a Lighttools Illumination system, consisting of dual Illumatool excitation systems (Lighttools Research, CA) coupled to a Hamatsu[®] CCD camera with excitation and emission filters for GFP (Lighttools Research). Images were captured and analyzed using QCapture software (Lighttools Research). For intratibial tumors, the GFP signal was typically detected at least 12 days following intratibial injection. In initial experiments to establish the relationship between in vivo imaging and histology of early tumors of varying sizes, animals with intratibial tumors

were sacrificed at days 0, 3, 5, 7, and 12 after initial tumor detection in the animal. Animals were sacrificed by cervical dislocation and autopsy performed aided by fluorescent imaging. Tumor bearing and non-tumor bearing rear legs were removed and evaluated.

Micro-CT Analysis

Prior to decalcification, trabecular and cortical bone content and character of fixed dissected tibias were analyzed by micro-CT imaging, using a Skyscan 1172 desktop microtomograph with high resolution capture and 3D modeling (Skyscan, Kontich, Belgium).

Bone Histology

Intact dissected tibias from individual mice were fixed in 10% neutral-buffered formaldehyde for 48 hr, followed by decalcification in 0.5 M EDTA for 4 days at 37°C. Serial sections (5 μ m) were cut using a Leica microtome. The locations of tumors were identified using hematoxylin and eosin staining. Serial sections containing tumor material were then analyzed for osteoclast activity by tartrate resistant acid phosphatase (TRAP) staining using standard procedures. Osteoblast numbers were also evaluated by standard histology.

RESULTS

Generation of PC3-GFP Cells and Isolation of Tumorigenic PC3-GFP Cells

Transfection of PC3 cells using pMaxGFP vector and selection on Geneticin resulted in the isolation of stable cell clones expressing GFP (Fig. 1a). Initial experiments using PC3-GFP cloned population of cells demonstrated limited capacity for growth *in vivo*, with tumors detected in some sub-cutaneous sites but not at intraosseous sites. Cells with a sub-cutaneous tumorigenic capacity *in vivo* were cultured *in vitro* from these sub-cutaneous tumors before re-implantation both at sub-cutaneous and intraosseous sites. Sub-cutaneous tumors were subsequently detected in 5/6 animals and intratibial tumors detected in 2/6 animals. Tumorigenic cells were again re-isolated from intraosseous tumors and after *in vitro* expansion, formed tumors in 6/6 animals when re-implanted into bone. Autopsy of animals with extensive osseous tumors also revealed the presence of para-aortic lymph node metastasis in all animals. These cells with affinity for growth in bone (termed PC3-GFP-Tib) generated from these implantations were frozen at low passage for use in later experiments.

Assessment of Tumor Growth at Early Time Points

To specifically identify very early stages of tumor growth, the highly tumorigenic PC3-GFP-Tib cells

were implanted into mice and tumors monitored daily. Some animals were sacrificed at early time points after initial observations of GFP-positive tumors in bone. In initial experiments animal cohorts were sacrificed at day 1 (the day tumors were first detected) and on days 3, 5, 7, and 12 after initial observation by GFP imaging. The majority of tumors identified by GFP imaging were initially visualized as apparently single lesions (Fig. 1b), although occasionally two fluorescent signals were detected that were later shown to be two separate clones by histology.

Histological Analysis of Osseous Lesions

Histological analysis of tumors from animals sacrificed on the first day after initial detection by GFP imaging revealed that the minimum resolution of *in vivo* imaging to be tumors of approximately 0.5–1 mm in diameter (Fig. 1b). Histological examination of osseous lesions revealed clear associations with observations by *in vivo* monitoring, revealing small tumors (<1 mm diameter) in animals sacrificed on day 1, and larger tumors present in animals sacrificed at later time point (Fig. 1b).

Detection of Tumors after Intracardiac Implantation

To assess whether PC3-GFP-Tib cells were able to home to bone, intracardiac injection was used. Tumors were detected by *in vivo* GFP-imaging, and all tumors detected after intracardiac injection targeted bone, affecting the tibia, scapulae, vertebrae, femur (Fig. 1c) as well as the skull.

Effects of Castration on Tumor Frequency and Time to Detection

The effect of castration on tumor frequency and size on days 6–9 after first detection was examined in animals that had been castrated 2 weeks prior to implantation compared to intact controls. A 2-week interval before implantation had been shown in previous studies to induce increased bone turnover in mice [9]. In addition, TRAP5c levels in serum in our animal groups increased markedly between weeks 2 and 3 after castration (data not shown) and remained elevated up to 5 weeks post-castration. In animals with tumors implanted directly into the tibia, there were no significant differences in the overall frequency (5/6 in both castrated and non-castrated groups), the time to first appearance of tumors (median day 15 vs. 18) or the final size of tumors ($\sim 4 \text{ mm}^3$) at autopsy (Fig. 2a,b). After intracardiac implantation, there was no difference in the total number of tumors (Fig. 2c) or time to

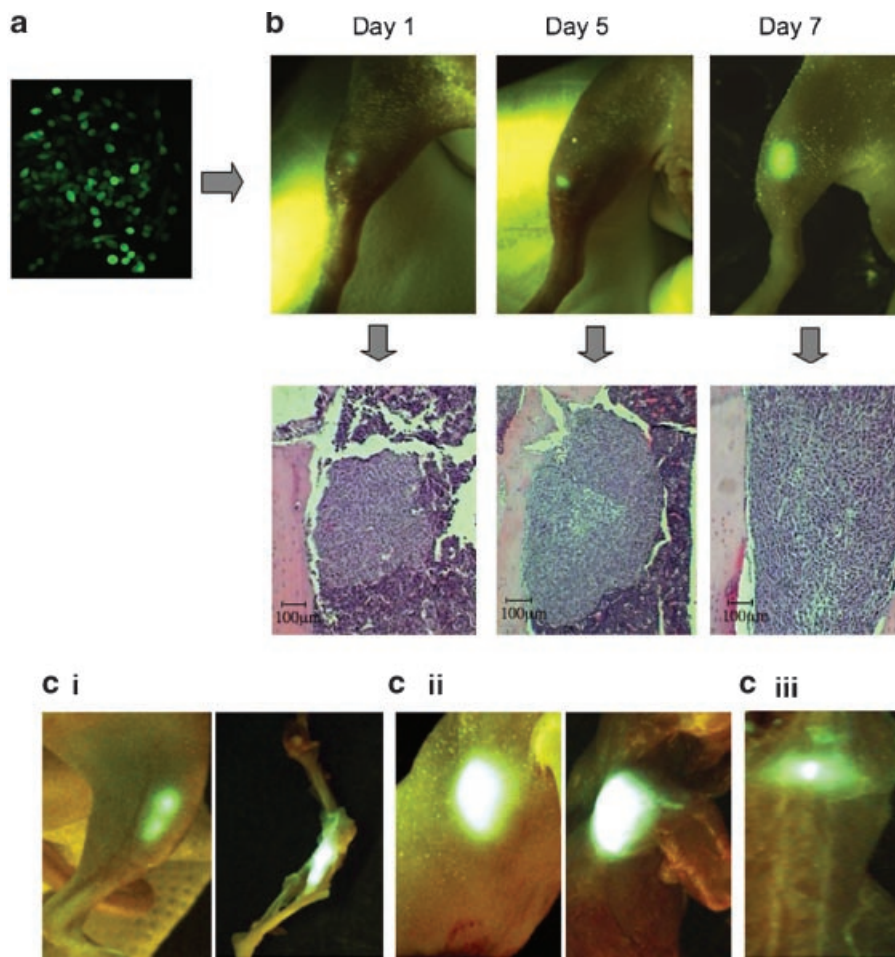


Fig. 1. **a:** Fluorescence microscopy of PC3-GFP cells growing in monolayer cell culture. **b:** Time course of tumor growth in tibias of a cohort of mice after intratibial implantation, sacrificed at various time points after tumors were first observed (day 1) and corresponding histology. **c:** Detection of tumors in live animals after intracardiac injection (i) Tibia in intact animal with corresponding image at autopsy, (ii) Scapula in intact animal with corresponding image at autopsy, and (iii) single vertebra at autopsy.

first appearance of tumors (Fig. 2d) between castrated and non-castrated groups.

Effect of Castration and/or the Presence of Tumor Cells on Bone Structure

Castration had clear and significant effects on trabecular bone volume and trabecular number in the non-tumor bearing legs (tibias) of animals at the time of sacrifice (Figs. 3 and Fig. 4a,b). The presence of the tumor in non-castrated animals, whether from intratibial or intracardiac injection, also reduced these parameters compared to contralateral bones (Fig. 4a–e). Cortical bone volume was also significantly ($P = 0.009$, *t*-test) reduced by castration in non-tumor bearing limbs but this effect was not observed in tumor bearing tibias (Fig. 4c). The presence of tumor in castrated animals did not have an additive effect over and above castration-induced changes.

Effect of Castration and/or the Presence of Tumor Cells on Bone and Bone Cell Populations

At the time of sacrifice, castration did not appear to affect osteoblast numbers, in the presence or absence of tumor cells, adjacent to either cortical bone or associated with the growth plate. The most significant effect on osteoblast numbers was induced by the presence of the tumor itself which very significantly suppressed osteoblast numbers in both castrated and intact animals (Fig. 5a). Osteoclast numbers were also not significantly affected by castration in the presence or absence of the tumor but were very significantly increased on cortical bone surfaces adjacent to tumor cells (Fig. 5b). Osteoclast numbers were also elevated at early time points (on the first day of detection by GFP-imaging) when tumors were still very small (<1 mm). The presence of the tumor within the tibia did not significantly affect either osteoblast or osteoclast numbers in the growth

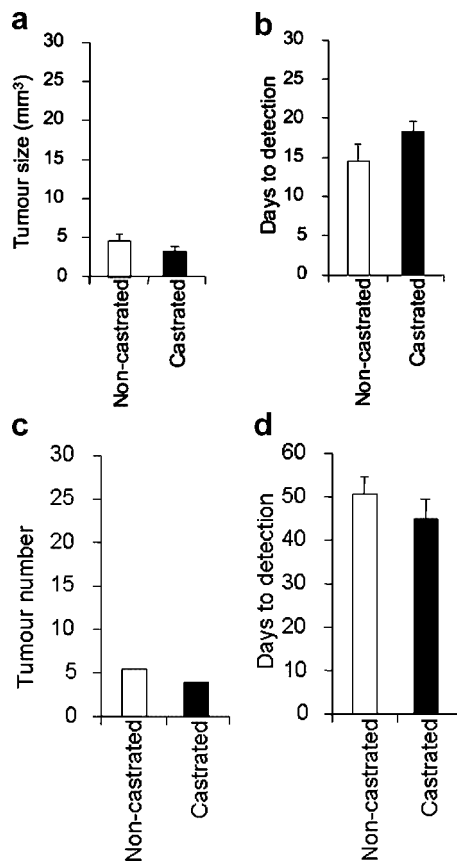


Fig. 2. (a) Comparison of the tumor size at sacrifice (days 6–9 after first observed) and (b) time to first observation of tumors by *in vivo* imaging in mice castrated 2 weeks prior to intratibial implantation compared to non-castrated controls. (c) Total number of tumors 1 week after first observation and (d) time to first observation after intracardiac implantation in mice castrated 2 weeks prior to intracardiac implantation, compared to non-castrated controls.

plate region, a location that was distant from the growing lesions in the diaphyses in all samples.

DISCUSSION

Our results clearly show that while castration produced significant effects on bone structure over the time courses of these experiments, indicative of increased bone turnover, this does not affect the growth rate of PC3 tumors or the frequency of tumor formation in bone. Detailed examination of bone structure indicated that the presence of the tumor itself had profound effects on bone turnover and on the numbers of osteoblasts and osteoclasts responsible for this activity. These results suggest that the effects of small numbers of tumor cells which suppress osteoblast activity and induce osteoclast activity, outweigh the effects of castration in modifying the bone microenvironment to the benefit of tumor growth in this model. This would suggest that at least in the case of PC3 cells, that preparing a “fertile soil” for tumor colonization, that is, one where there is enhanced bone turnover when the tumor cells are inoculated, does not predispose bone to tumor colonization. This is an interesting observation given that another study has suggested that modifying the bone microenvironment at the time of implantation can enhance tumor metastasis frequency in animals inoculated with PC3 cells by intracardiac injection [4]. It should be noted that in the latter study in which cells were inoculated by intracardiac injection, tumors did form in both intact and in bisphosphonate treated animals with relatively suppressed bone turnover, albeit at a lower rate to that observed in PTH treated animals, so it may be that different environments favor the growth of cell clones with distinct characteristics [4]. In the present study the PC3-GFP cells were cloned twice before injection so were essentially monoclonal. In addition, direct effects of PTH on tumor growth could

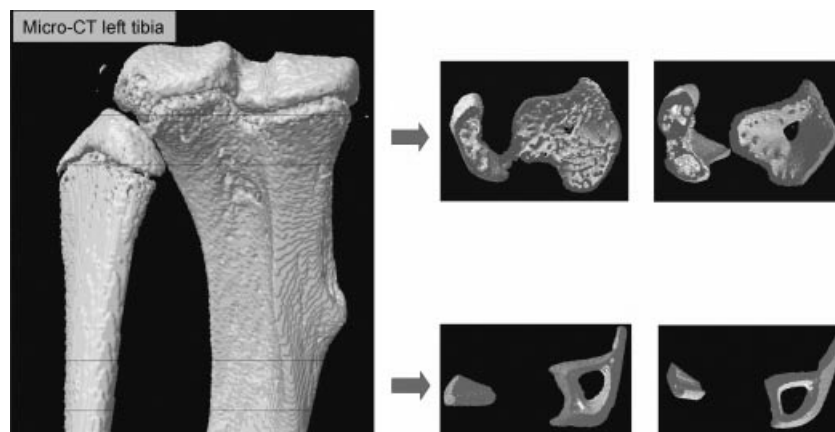


Fig. 3. Example of typical micro-CT scans of non-tumor bearing tibias showing loss of trabecular structure in the growth plate region (standard measurement in all samples: 200 μ m below the growth plate, analysis: 1 mm) and cortical region (analysis starting 1 mm from growth plate, analysis: 1 mm) of tibias from intact (left transverse section) versus castrated (right transverse section) animals at the time of sacrifice (days 6–8).

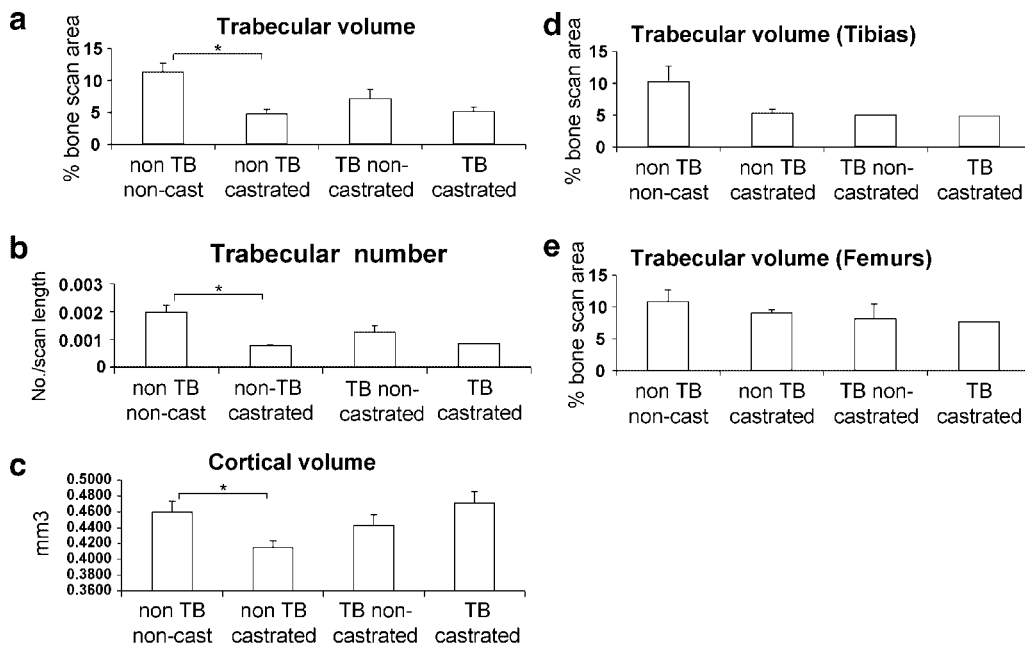


Fig. 4. (a) Comparison of total trabecular volume as a percentage of total bone volume and (b) trabecular number in a standard cross-sectional scan through the growth plate region (standard measurement in all samples: starting 200 μm below the growth plate, analysis: 1 mm), of tibias from sacrificed animals (days 6–9 after tumor first observed) that had been castrated 2 weeks before intratibial tumor implantation versus tibia scans from intact controls (*significant at $P < 0.005$, t -test $n = 4-6$). (c) Comparison of cortical bone thickness in a standard cross-sectional scan through the tumor associated cortical bone ((standard measurement in all samples: cortical region (starting 1 mm from growth plate, analysis: 1 mm)) in tibias from sacrificed animals (days 6–9 after tumor first observed) that had been castrated 2 weeks before intratibial tumor implantation versus tibia scans from intact controls (*significant at $P < 0.009$, t -test, $n = 4-6$). (d) Comparison of total trabecular volume from tibias and (e) from femurs following intracardiac implantation in castrated and non-castrated animals in bone versus intact controls (standard measurement in all samples: starting 200 μm below the growth plate, analysis of 1 mm).

account for increased tumor frequency in animals with increased bone turnover.

Bone histomorphometry demonstrated that tumors induced bone loss in non-castrated animals, whereas presence of tumor did not induce additional bone loss in castrated animals. This lack of additive effect is likely to be the result of early sacrifice of animals at time points when tumors were still small, and castration-induced changes on bone structure predominated. Tumor cells implanted by the intratibial route generally formed tumors away from the growth plate where their presence significantly affected osteoclast and osteoblast numbers (Fig. 5). Bone histomorphometry of trabecular bone (distal to the tumor) did show moderate but not significant levels of bone loss. It is likely that effects on trabecular bone due to presence of tumor in castrated animals would be more pronounced and become significant in more advanced tumors, however this remains to be tested.

PC3 cells are highly tumorigenic in mice, and induce osteoclast activation, coupled with inhibition of osteoblast activation when grow in bone, resulting in tumors that are highly osteolytic. This phenotype in bone does differ from the majority of prostate cancer metastases to

bone, which are generally osteosclerotic, although tumor induced bone remodeling is thought to implicitly involve underlying osteolytic activity. PC3 cells were used in this study since they do not respond directly to androgens, being androgen receptor null. The use of this model allowed us to assess the indirect effects of androgen withdrawal on tumor growth mediated via action in the bone microenvironment in the absence of direct effects on tumor cell growth. In addition PC3 cells readily colonize bone in xenograft models and target bone following intracardiac injection. In this study we show that osteoclast recruitment and/or activation occurs early during prostate cancer cell growth in bone, consistent with the activities observed in prostate cancers where simultaneously dysregulating bone formation and resorption is a characteristic. Since osteoclastogenesis takes around 7 days in vitro, and increased numbers of osteoclasts were seen within 12 days of implantation, induction of osteoclast differentiation must occur soon after tumor implantation. The factors derived from PC3 cells that drive this inductive process have yet to be determined, however we do know that these cells produce biologically active levels of osteoprotegerin (OPG) and

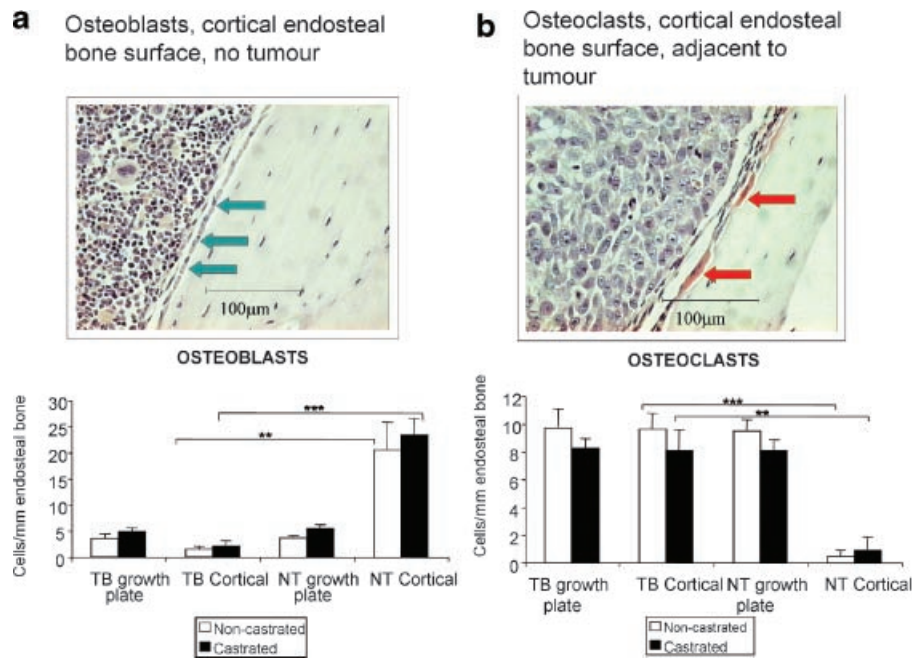


Fig. 5. **a:** Light micrograph of a section of tibia showing osteoblasts, identified morphologically, (green arrows) and corresponding analysis of osteoblast numbers in tumor bearing (TB) and non-tumor bearing (NT) tibias from sacrificed animals (days 6–9 after tumor first observed) that had been castrated 2 weeks before intratibial implantation versus intact controls (*significant at $P < 0.005$, *t*-test). **b:** Light micrograph of a section of tibia showing osteoclasts, identified by TRAP staining (red arrows), and corresponding analysis of osteoclast numbers in tumor bearing (TB) and non-tumor bearing (NT) tibias from sacrificed animals (days 6–9 after tumor first observed) that had been castrated 2 weeks before tumor implantation versus intact controls (*significant at $P < 0.005$, *t*-test).

express only low levels of RANKL (receptor activator of NF κ B ligand) in vitro [10]. The latter molecule, RANKL, expressed on the surface of osteoblasts has been shown to bind RANK on osteoclast precursors and induce their differentiation to mature osteoclasts [11]. OPG has antagonist activity in this system, binding RANKL and suppressing osteoclastogenesis [12]. If PC3 cells involved in the formation of tumors in vivo retained the ability to produce OPG, the increased numbers of osteoclasts observed in the lesions described in the present study would be paradoxical, however we have consistently shown that PC3 cells that selectively form tumors in bone do not produce biologically active amounts of OPG when re-isolated in vitro (data not shown). This is an interesting observation and highlights the selective nature of tumor growth in particular environments leading to the emergence to cell populations with adapted characteristics. The suppression of osteoblast numbers and resulting osteolytic lesions induced by the presence of PC3 cells is likely to be due, in part, to the high levels of the Wnt antagonist, DKK1 (Dickkopf 1) shown by us and others [13] to be expressed by this cell line. DKK1 is an antagonist of Wnt-frizzled signaling, shown to induce osteoblast differentiation in mesenchymal progenitors, and therefore inhibits the maturation of osteoblasts and bone formation.

Direct injection of tumor cells into the tibia has been successfully used to study biochemical interactions of tumor cells and the bone microenvironment and mimic events leading to tumor establishment in bone [8]. This approach however does not model tumor trafficking to bone, extravasation and migration [14–16]. In this study, we have used both intratibial injection, and intracardiac injection, to mitigate effects of bone disruption caused by injection into bone, and to assess, via the circulation, tumor colonization of bone in castrated and non-castrated animals. The use of GFP for monitoring tumor growth used in the present study does add new possibilities for the study of early growth of tumors in bone allowing sacrifice of animals at specific time points after colonization of bone, and whilst tumors are still very small. This is particularly relevant to intracardiac injections, where the location and time of tumor presentation is not predictable. GFP-monitoring of prostate tumor cell growth in intratibial xenograft tumors has been reported previously [7,17], however these studies did not address early tumor growth, and imaging was used to assess the effects of bisphosphonate treatment on tumors up to 8 weeks after injection, at which point tumors were $>1\text{ cm}^3$ in the majority of tumor bearing mice. Using GFP in our study, it was possible to detect tumors in bone at much earlier time-points than previously reported [7,17–19], facilitating the evaluation

of tumor-induced changes to the bone microenvironment, and potentially targeting of tumor growth in bone prior to the establishment of extra-osseous growth. In the present study, we show that GFP-positive PC3 tumors can be detected in bone as early as 12 days after intratibial implantation, and are first detected when they reach a diameter of approximately 0.5–1 mm. Recent studies using GFP-imaging of prostate cancer growth in bone detected similar sized tumors, but only after *ex vivo* imaging of dissected tibias [18]. The present study therefore further defines the potential resolution for GFP-based monitoring of tumor growth in bone in live animals. As shown herein, direct visualization of tumors in bone at early stages of tumor growth allows studies to be undertaken using tumors within a limited size range during the period of their establishment, and prior to overt bone destruction, rather than when they have developed extra-osseous disease [7,17].

In summary, in the present study we have described a GFP-based model of prostate cancer tumor growth in bone, which further defines the limits of detection of GFP-based *in vivo* monitoring of tumor growth in bone, and in which we demonstrate that castration does not affect the incidence of tumor formation or their growth rate. We have also shown that the presence of the tumor cells themselves have profound effects at an early stage on cells involved in bone turnover potentially shifting the balance within lesions to one where lysis predominates. However at the time of sacrifice this shift did not appear to have a significant impact on measured parameters of bone structure. In the context of the castration results, where clear evidence of bone loss was observed, bone lysis *per se* does not increase tumor growth/survival in this model. In addition, we have shown that small tumors can be reliably detected in bone using fluorescent *in vivo* imaging, and suggest that this technology will facilitate studies targeting of prostate cancer–bone interactions when lesions are at an early stage of development.

ACKNOWLEDGMENTS

We thank Dr. Les Coulton for assistance with Micro-CT analysis. This work was funded by Yorkshire Cancer Research and a grant from the MRC (PROMPT) and a European Union FP6 Award (PRIMA).

REFERENCES

- Saitoh H, Hida M, Shimbo T, Nakamura K, Yamagata J, Satoh T. Metastatic patterns of prostatic cancer: Correlation between sites and number of organs involved. *Cancer* 1984;54:3078–3084.
- Bubendorf L, Schöpfer A, Wagner U, Sauter G, Moch H, Willi N, Gasser TC, Mihatsch MJ. Metastatic patterns of prostate cancer: an autopsy study of 1,589 patients. *Hum Pathol* 2000;31:578–583.
- Moreno JG, Croce CM, Fischer R, Monne M, Vihko P, Mulholland SG, Gomella LG. Detection of hematogenous micrometastasis in patients with prostate cancer. *Cancer Res* 1992;52:6110–6112.
- Schneider A, Kalikin LM, Mattos AC, Keller ET, Allen MJ, Pienta KJ, McCauley LK. Bone turnover mediates preferential localization of prostate cancer in the skeleton. *Endocrinology* 2005;146:1727–1736.
- Yang M, Jiang P, Yamamoto N, Li L, Geller J, Moossa AR, Hoffman RM. Real-time whole-body imaging of an orthotopic metastatic prostate cancer model expressing red fluorescent protein. *Prostate* 2005;6:374–379.
- Kalikin LM, Schneider A, Thakur MA, Fridman Y, Griffin LB, Dunn RL, Rosol TJ, Shah RB, Rehemtulla A, McCauley LK, Pienta KJ. *In vivo* visualization of metastatic prostate cancer and quantitation of disease progression in immunocompromised mice. *Cancer Biol Therapy* 2003;2:656–660.
- Burton DW, Geller J, Yang M, Jiang P, Barken I, Hastings RH, Hoffman RM, Deftos LJ. Monitoring of skeletal progression of prostate cancer by GFP imaging, X-ray, and serum OPG and PTHrP. *Prostate* 2005;62:275–281.
- Corey E, Quinn JE, Bladou F, Brown LG, Roudier MP, Brown JM, Buhler KR, Vessella RL. Establishment and characterisation of osseous prostate cancer models: intratibial injection of human prostate cancer cells. *Prostate* 2003;52:20–33.
- Vanderschueren D, Vandenput L, Boonen S, Lindberg MK, Bouillon R, Ohlsson C. Androgens and bone. *Endocrine Rev* 2004;25:389–425.
- Holen I, Croucher PI, Hamdy FC, Eaton CL. Osteoprotegerin (OPG) is a survival factor for human prostate cancer cells. *Cancer Res* 2002;62:1619–1623.
- Khosla S. Minireview: The OPG/RANKL/RANK system. *Endocrinology* 2001;142:5050–5055.
- Emery JG, McDonnell P, Burke MB, Deen KC, Lyn S, Silverman C, Dul E, Appelbaum ER, Eichman C, DiPrinzio R, Dodds RA, James IE, Rosenberg M, Lee JC, Young PR. Osteoprotegerin is a receptor for cytotoxic ligand TRAIL. *J Biol Chem* 1998;273:14363–14367.
- Hall CL, Bafico A, Dai J, Aaronson SA, Keller ET. Prostate cancer cells promote osteoblastic bone metastases through Wnts. *Cancer Res* 2005;65:7554–7560.
- Singh AS, Figg WD. *In vivo* models of prostate cancer metastasis to bone. *J Urol* 2005;174:820–826.
- Angelucci A, Gravina GL, Rucci N, Festuccia C, Muzi P, Vicentini C, Teti A, Bologna M. Evaluation of metastatic potential in prostate carcinoma: an *in vivo* model. *Int J Oncol* 2004;25:1713–1720.
- Nemeth JA, Harb JF, Barroso U Jr, He Z, Grignon DJ, Cher ML. Severe combined immunodeficient-hu model of human prostate cancer metastasis to human bone. *Cancer Res* 1999;59:1987–1993.
- Yang M, Burton DW, Geller J, Hillegonds DJ, Hastings RH, Deftos LJ, Hoffman RM. The bisphosphonate olpadronate inhibits skeletal prostate cancer progression in a green fluorescent protein nude mouse model. *Clin Cancer Res* 2006;12:2602–2606.
- Yamamoto H, Bonfil RD, Wiesner C, Nabha S, Dong Z, Meng H, Saliganan A, Sabbota A, Chinni SR, Cher ML. Quantitative assessment of small intraosseous prostate cancer burden in SCID mice using fluorescence imaging. *Prostate* 2007;67:107–114.
- Yang M, Baranov E, Moossa AR, Penman S, Hoffman RM. Visualizing gene expression by whole-body fluorescence imaging. *Proc Natl Acad Sci USA* 2000;97:12278–12282.